RAPID COMMUNICATIONS

# PHYSICAL REVIEW C

## NUCLEAR PHYSICS

THIRD SERIES, VOLUME 51, NUMBER 6 JUNE 1995

## RAPID COMMUNICATIONS

*The Rapid Communications section is intended for the accelerated publication of important new results. Manuscripts submitted to this section are given priority in handling in the editorial office and in production. A Rapid Communication in* **Physical Review C** *may be no longer than five printed pages and must be accompanied by an abstract. Page proofs are sent to authors.*

# Yrast bands in $^{117}$I and $^{116-118}$Xe: Anomalous quasiparticle alignment frequencies and band termination

E.S. Paul,[1] D.B. Fossan,[2] K. Hauschild,[3] I.M. Hibbert,[3] H. Schnare,[2] J.M. Sears,[2] I. Thorslund,[2] R. Wadsworth,[3] A.N. Wilson,[1] and J.N. Wilson[1]

[1]*Oliver Lodge Laboratory, University of Liverpool, P.O. Box 147, Liverpool L69 3BX, United Kingdom*

[2]*Department of Physics, State University of New York at Stony Brook, Stony Brook, New York 11794*

[3]*Department of Physics, University of York, Heslington, York YO1 5DD, United Kingdom*

(Received 10 March 1995)

The yrast bands of neutron-deficient $^{117}$I and $^{116}$Xe have been extended to $I \sim 34\hbar$, and $^{117,118}$Xe to $I \sim 46\hbar$, using highfold $\gamma$-ray coincidence data collected with the Eurogam II spectrometer. Systematic quasiparticle alignment frequencies are discussed and compared to theoretical cranked Woods-Saxon calculations. The first pair alignment is attributed to $h_{11/2}$ protons despite theoretical expectations for $h_{11/2}$ neutron alignment; the neutron alignment appears significantly delayed. At higher spins, the $^{117}$I and $^{117}$Xe isobars exhibit contrasting forms of band termination.

PACS number(s): 21.10.Re, 27.60.+j, 23.20.Lv

The lowest-frequency quasiparticle pair alignments in nuclei of mass $A \sim 120$ have generally been attributed to the rotational alignment of $h_{11/2}$ neutrons. This conclusion has been mainly based on comparison with theory, namely the cranking model, which has previously described the properties of pair alignments quite well. However, with new systematic experimental data extending to high spin, discrepancies have become apparent between theory and experiment. For example, analysis of experimental data for the lightest neutron-deficient nuclei of the $A \sim 120$ region has suggested that $h_{11/2}$ *protons* are responsible for the first pair alignments, e.g., Refs. [1,2]. In this paper, new results, obtained with the Eurogam II spectrometer, are presented for the yrast bands in even-even $^{116,118}$Xe, odd-$N$ $^{117}$Xe, and odd-$Z$ $^{117}$I. The observed pair alignment frequencies are discussed and compared to theoretical expectations based on the cranking model. It is proposed that the first pair alignment in these nuclei is due to protons, and that the neutron alignment is significantly delayed. At higher spins, the influence of oblate configurations is expected in these nuclei which lie just above the $Z=50$ shell closure. Contrasting behavior is found for $^{117}$I and $^{117}$Xe at high spin. Both show evidence for band termination; yrast noncollective states compete with the rotational states in $^{117}$I, while the characteristics of the yrast band in $^{117}$Xe are those associated with a form of "smooth" termination in which a gradual shape change from prolate to oblate occurs over many transitions [3].

$\gamma$-rays emitted following the $^{31}$P+$^{90}$Zr reaction have been studied at the Centre de Recherches Nucléaires, Strasbourg, using the Eurogam II spectrometer [4] which contains 54 Compton-suppressed HPGe detectors including 24 segmented (four-element) "clover" detectors [5]. The Vivitron electrostatic accelerator provided a 150-MeV $^{31}$P beam to bombard two stacked self-supporting foils of $^{90}$Zr ($>97\%$ enriched), each of nominal thickness 440 $\mu$g/cm$^2$. High-spin states in $^{117}$I were populated via the strong $2p2n$ exit channel, while states in $^{116-118}$Xe were populated via $pxn$ channels ($x=2-4$). Many other reaction channels, however, were also populated with significant strength, namely the $^{115,116}_{53}$I, $^{114-117}_{52}$Te, and $^{113,114}_{51}$Sb nuclides.

Approximately $8.5\times10^8$ highfold $\gamma^n$ coincidence events ($n \geq 5$) were accumulated in 48 hours of beam time. These data were unfolded off-line into triple coincidence events ($1.3\times10^{10}$ such events) and incremented into a "radware" cube [6] with a nonlinear gain compression of 2 channels/full width at half maximum. In this way, $\gamma$ rays with energies

 © 1995 The American Physical Society

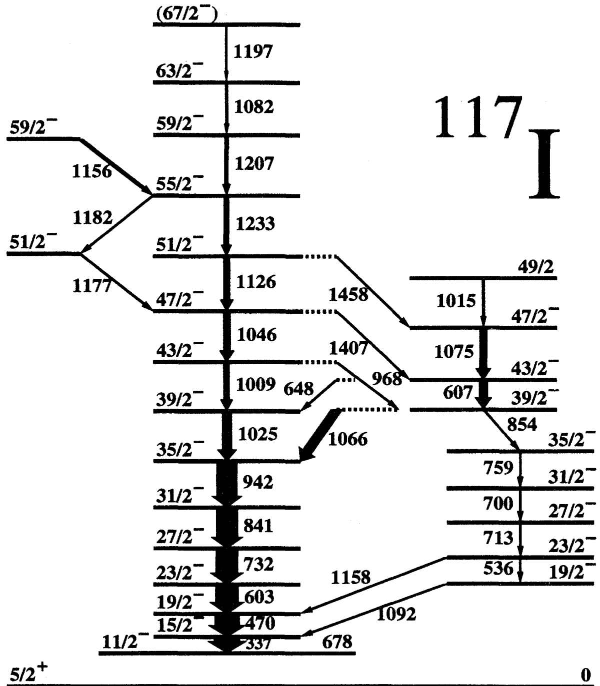


FIG. 1. Partial decay scheme of $^{117}$I.

between 100 keV and 3 MeV were stored in the cube which had 1193 channels per dimension (the cube was symmetrized such that only 1/6 needed to be stored requiring 0.59 Gbyte of disk storage). Analysis was facilitated with the LEVIT8R graphical analysis package [6] where double-gated one-dimensional (1D) $\gamma$-ray spectra could readily be projected out of the cube. This analysis of triple coincidence data was essential due to the large number of nuclides produced in the present reaction. Finally, after chains of mutually coincident $\gamma$ rays were established, the original data were unfolded directly into 1D spectra with gating conditions of two, three, and four $\gamma$ rays from a list of energies (typically 10 coincident $\gamma$ rays) [7]. This greatly enhanced the weak structures in the data such as weakly populated exit channels (e.g., $^{116}$Xe) and high-spin rotational sequences in the stronger channels. Furthermore, the quality of spectra obtained from triple- (quadruple-) gated events was markedly improved (less contamination) compared to double-gated spectra obtained from the cube. Each increase in gating fold, however, decreased the statistics by an order of magnitude.

In order to determine the multipolarities of $\gamma$-ray transitions, the coincidence data were sorted into an angular correlation matrix of clover detectors ($70° \leq \theta \leq 110°$) on one axis against forward/backward detectors ($\theta = 22°/158°$) on the other axis. Intensity ratios obtained from this matrix were used to determine between stretched dipole and stretched quadrupole transitions using the DCO method (directional correlation of oriented states) [8]. Furthermore, the electric or magnetic nature of transitions could be determined by measuring $\gamma$-ray linear polarizations using the segmented clover detectors as Compton polarimeters [5].

Figure 1 shows the negative-parity states in $^{117}$I including the yrast band [9] which has been extended up to $I^\pi = (67/2^-)$ (note that the 1009 and 1046 keV transitions have been reordered from Ref. [9]). The spin/parity assignments for all the levels in the yrast band from $11/2^-$ up to $63/2^-$ are based on measured $\gamma$ ray angular correlation ratios and $\gamma$-ray linear polarizations obtained from the present data set. These results are consistent with electric quadrupole transitions, with an average linear polarization $P \sim 0.4$ (previously, only the quadrupole nature of transitions up to $I^\pi = 39/2^-$ could be established [9]). Figure 2 shows spectra generated for the yrast bands of $^{116,118}$Xe by demanding at least four mutually coincident transitions as gates within an event, and the yrast band of $^{117}$Xe by demanding at least three mutually coincident gates. The yrast band of $^{116}$Xe [10] has been significantly extended from $I^\pi = 18^+$ to a tentative spin $I^\pi = (34^+)$. The band is too weak for reliable angular correlation and linear polarization values to be extracted for the new transitions. The yrast band of $^{118}$Xe [1] has also been extended [above the 1311 keV $36^+ \rightarrow 34^+$ transition of Fig. 2b)], and in this case it was possible to establish the electric quadrupole nature of the transitions up to and including the 1311 keV $\gamma$ ray from the angular correlation and linear polarization measurements. It can be clearly seen in Fig. 2(b) that four $\gamma$ rays are bunched together at $E_\gamma \sim 1270$ keV (1260, 1269, 1281, and 1286 keV). Only three of these four transitions were placed in the yrast band of $^{118}$Xe presented in Ref. [1]. The topmost clear transition in the present work is the 1420 keV $\gamma$-ray depopulating a state with tentative spin $I^\pi = (40^+)$. Higher energy transitions, however, can be seen in the spectrum and a suggested continuation of the band is through the 1477, 1523, and 1615 keV transitions reaching a tentative spin of $I^\pi = (46^+)$. Finally, the yrast band of $^{117}$Xe [1] has been extended from $I^\pi = 47/2^-$ to a tentative spin $I^\pi = (91/2^-)$ as shown in Fig. 2(c). It was only possible to extract reliable angular correlation information up to $I^\pi = 47/2^-$.

The experimental alignments $i_x$ [11] of the yrast bands in $^{116,118}$Xe are shown in Fig. 3 as a function of rotational frequency, together with the yrast $\nu h_{11/2}$ band in $^{117}$Xe and the yrast $\pi h_{11/2}$ band in $^{117}$I. A variable moment of inertia reference, with Harris parameters [12] $\mathscr{J}_0 = 15\hbar^2$ MeV$^{-1}$ and $\mathscr{J}_1 = 25\hbar^4$ MeV$^{-3}$, has been subtracted. The yrast band of $^{118}$Xe shows a sharp alignment gain at $\omega_1 = 0.39$ MeV/$\hbar$ and a second at $\omega_4 \approx 0.65$ MeV/$\hbar$. The yrast band of $^{116}$Xe also shows two, more gradual, gains in alignment. The first occurs at the same frequency as that in $^{118}$Xe, while the second is somewhat lower in frequency ($\omega_3 = 0.51$ MeV/$\hbar$) and shows a lower alignment gain. The yrast $h_{11/2}$ bands in neighboring odd-$N$ $^{117}$Xe and odd-$Z$ $^{117}$I do not show the alignment at $\omega_1 = 0.39$ MeV/$\hbar$. Instead, $^{117}$Xe backbends at $\omega_2 = 0.46$ MeV/$\hbar$, while $^{117}$I backbends at $\omega_3 = 0.51$ MeV/$\hbar$ (the same frequency as the second alignment in $^{116}$Xe). At higher frequencies, an abrupt backbend occurs at $\omega_4 \approx 0.60$ MeV/$\hbar$ in $^{117}$I.

In order to investigate the theoretical aspects of the quasiparticle pair alignments evident in Fig. 3, calculations based on the cranking model have been performed. Total Routhian surface (TRS) calculations [14–16] predict prolate shapes for $^{116,118}$Xe at low spin with deformation parameters $\beta_2 \approx 0.22$, $\gamma \approx 0°$ ($^{116}$Xe) and $\beta_2 \approx 0.23$, $\gamma \approx 0°$ ($^{118}$Xe), respectively. Similarly, deformation parameters $\beta_2 \approx 0.22$,

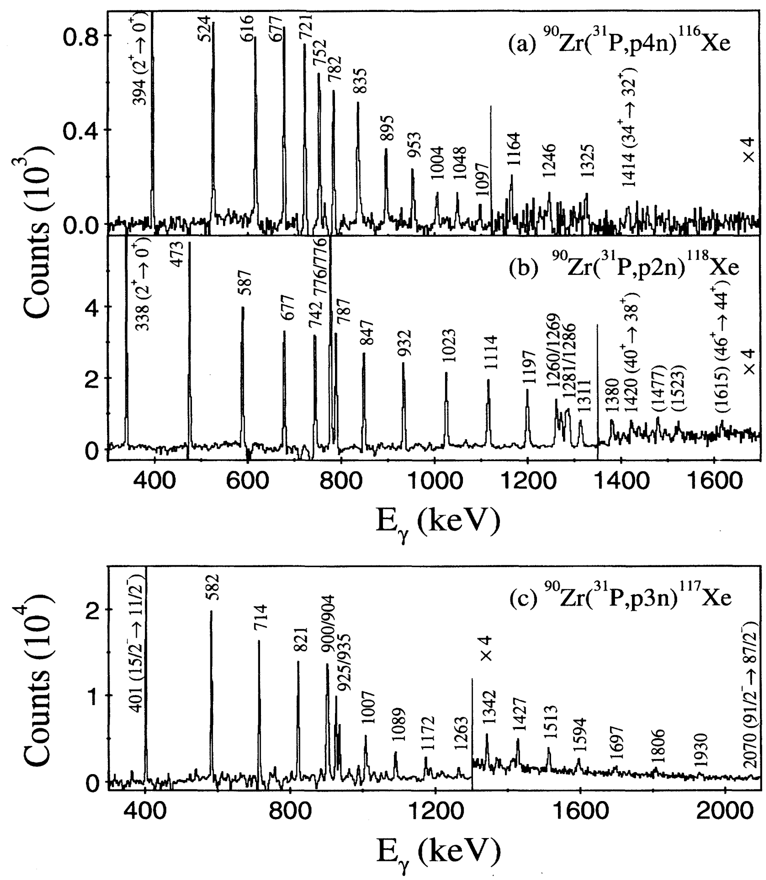


FIG. 2. $\gamma$ rays in simultaneous coincidence with any four of the strongest yrast transitions in (a) $^{116}$Xe and (b) $^{118}$Xe. Triple-gated spectra have been used as background spectra. $\gamma$ rays in simultaneous coincidence with any three of the strongest yrast transitions in (c) $^{117}$Xe.

$\gamma \approx -10°$ are predicted for the yrast $\nu h_{11/2}$ band of $^{117}$Xe, and $\beta_2 \approx 0.21$, $\gamma \approx +10°$ for the yrast $\pi h_{11/2}$ band of $^{117}$I. These deformation parameters have been used as input to cranked Woods-Saxon calculations in order to obtain theoretical quasiparticle pair alignment frequencies, specifically for neutrons and protons from the $h_{11/2}$ subshell. An example is shown in Fig. 4 for the $^{116}$Xe deformation parameters, where the negative-parity Routhians intruding from the $h_{11/2}$ subshell are labeled by $e$, $f$ for neutrons and $E$, $F$ for protons, respectively. In these cranking calculations, the pairing strength has been calculated at zero frequency and made to decrease with increasing rotational frequency such that the

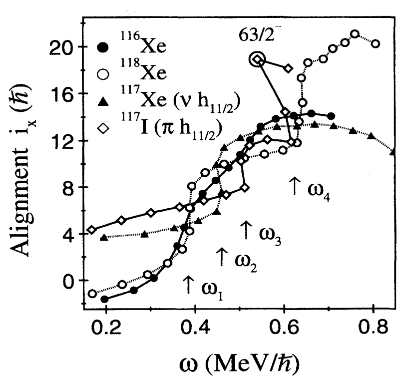


FIG. 3. Alignment $i_x$ vs rotational frequency $\omega$.

pairing has fallen by 50% at $\omega = 0.70$ MeV/$\hbar$ (details can be found in Ref. [14]). The TRS calculations show small changes in deformation ($\beta_2$ and $\gamma$) associated with the various quasiparticle alignments, which reflect polarization effects of the aligning particles on the core (results for several quasiparticle configurations in $^{118}$Xe can be found in Ref. [1]). No significant difference is, however, found for the neutron $\omega_{ef}$ alignment frequency with these small changes in the deformation parameters. In fact, this alignment frequency is constant for $\gamma$ in the range $-10° \leq \gamma \leq +10°$. The corresponding proton $\omega_{EF}$ alignment frequency is more sensitive to changes in both $\beta_2$ and $\gamma$. For example, with $\beta_2 = 0.22$, the alignment frequency changes from 0.44 MeV/$\hbar$ for $\gamma = -10°$ to 0.39 MeV/$\hbar$ for $\gamma = +10°$.

The heavier even xenon isotopes $^{120-126}$Xe all show an alignment at $\omega_1 \approx 0.39$ MeV/$\hbar$ progressing from an upend to a backbend (e.g., Ref. [1]). However, as pointed out in Ref. [1], extra alignment is gained in the cases of $^{118}$Xe and $^{120}$Xe, which suggests differing aligning particles for the lighter and heavier Xe isotopes; indeed, neutron alignment is expected in the heavier isotopes, while proton alignment is suggested for the lighter isotopes. If protons are responsible for the first alignment, then one would expect this alignment to also occur in odd-$N$ $^{117}$Xe at a similar frequency (i.e., $\omega_1 \approx \omega_2$). In contrast, $\omega_2$ is delayed by 60 keV (20%). This delay can, however, be understood, with reference to the cranking calculations discussed above, as caused by the shape differences of the prolate $^{116,118}$Xe bands ($\gamma \sim 0°$)

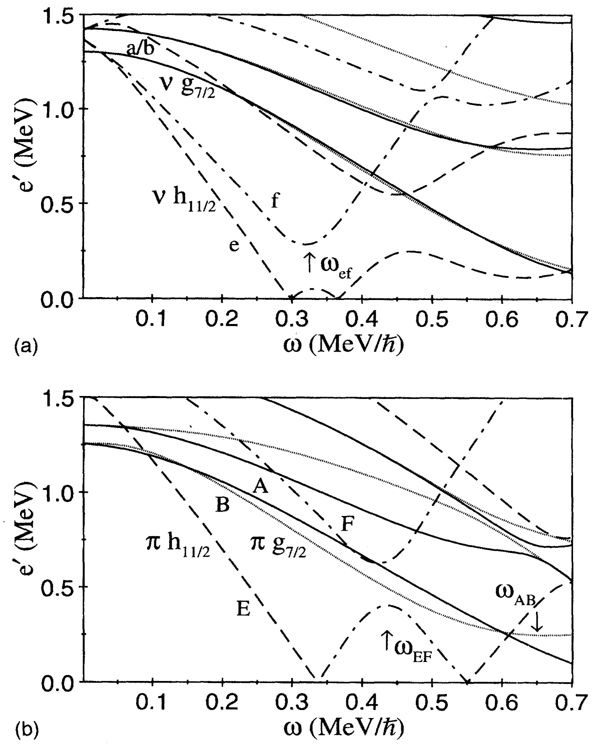


FIG. 4. Representative cranked Woods-Saxon Routhians for (a) neutrons and (b) protons calculated with deformation parameters $\beta_2=0.220$, $\beta_4=0.035$, and $\gamma=0°$. The parity and signature $(\pi,\alpha)$ of the levels are (+,+1/2), solid lines; (+,–1/2), dotted lines; (–,–1/2), dashed lines; (–,+1/2), dot-dashed lines. Quasiparticle alignment frequencies for neutrons $(\omega_{ef})$ and protons $(\omega_{EF},\omega_{AB})$ are indicated.

compared to the triaxial $^{117}$Xe band $(\gamma\sim-10°)$. The yrast band in odd-$Z$ $^{117}$I does not show the proton alignment at $\omega_1$ since it is blocked by the occupation of a single $h_{11/2}$ orbital by the odd proton.

With the first quasiparticle alignment $\omega_1$ ($\omega_2$ in $^{117}$Xe) attributed to protons, the quasiparticle alignment $\omega_3$ can then be attributed to $h_{11/2}$ neutrons. This alignment occurs at the same frequency in both $^{116}$Xe and $^{117}$I, and is blocked in $^{117}$Xe, as expected. It does however appear to be lacking, or significantly delayed to $\omega_4$ by 140 keV (27%), in $^{118}$Xe. This interpretation of proton alignment followed by neutron alignment is contrary to the cranking calculations of Fig. 4. Here the *neutron* $\omega_{ef}$ alignment, which is insensitive to modest changes in nuclear shape, occurs at a much lower frequency than the *proton* $\omega_{EF}$ alignment. The proton alignment needs to be reduced slightly (10%) such that $\omega_1=\omega_{EF}$ [the calculations of Fig. 4(b) are for $\gamma=0°$]. The neutron alignment must however be significantly delayed in frequency (55%) such that $\omega_3=\omega_{ef}$.

Several possibilities for a delayed neutron alignment in $^{117}$I have been addressed in Ref. [13]. For example, delayed particle alignments in odd-$A$ nuclei have been attributed to a strong quadrupole-quadrupole neutron-proton interaction between the aligning particles and low $\Omega$ intruder orbitals [17,18]. This mechanism, which is absent in the cranking calculations, is especially favored when the valence protons and neutrons have a large spatial overlap. This is the case for the neutron-deficient iodine isotopes where the odd proton occupies the $\pi h_{11/2}[550]1/2^-$ Nilsson orbital and low $\Omega$ $h_{11/2}$ neutrons align. A strong neutron-proton interaction is able to produce a strong mixing between the one-quasiparticle band below the alignment and the three-quasiparticle band above. Consequently, the alignment is delayed and smoothed out [19]. However, in contrast, a sharp backbend is seen for $^{117}$I ($\omega_3$) suggesting little mixing between the $\pi h_{11/2}$ and $\pi h_{11/2}\otimes[\nu h_{11/2}]^2$ configurations.

A large increase in $i_x$ and backbend is observed for the second alignment in $^{117}$I ($\omega_4$). A gradual alignment of $g_{7/2}$ protons [$\omega_{AB}$ in Fig. 4(b)] is expected at about the right frequency. However, such a sharp backbend is not expected and the alignment gain is too large. Instead, the low-lying $63/2^-$ state (Fig. 1) may represent the termination of this band into a noncollective oblate shape $(\gamma=+60°)$ based on the $\pi[h_{11/2}g_{7/2}^2]_{23/2^-}\otimes\nu[h_{11/2}^4(g_{7/2}/d_{5/2})^{10}]_{20^+}$ configuration relative to the $N=Z=50$ doubly magic core. Such a state is predicted to be yrast in $^{117}$I [9] and a corresponding state is observed in neighboring $^{115}$I [20]. Similarly, the $39/2^-$ and (yrast) $43/2^-$ states, shown to the right in Fig. 1, have been interpreted as noncollective oblate states based on $\pi[h_{11/2}g_{7/2}^2]_{23/2^-}\otimes\nu[h_{11/2}^4(g_{7/2}/d_{5/2})^{10}]_{8^+,10^+}$ configurations, respectively [13]. The bunching together of the $\gamma$-ray transitions in $^{118}$Xe ($E_\gamma\sim1270$ keV) at the second alignment, and the consequent extremely high alignment frequency ($\omega_4\approx0.65$ MeV/$\hbar$), were originally taken as evidence for a similar band termination in $^{118}$Xe [21]. Indeed, TRS calculations indicate an yrast noncollective state at $I^\pi=36^+$ based on the $\pi[h_{11/2}^2g_{7/2}^2]_{16^+}\otimes\nu[h_{11/2}^4(g_{7/2}/d_{5/2})^{10}]_{20^+}$ configuration [1] (closely related to the $63/2^-$ state in $^{117}$I). However, with the new data, the yrast band is seen to continue smoothly through the alignment and is best interpreted as a normal pair alignment in a prolate nucleus. The observed alignment gain is again too large for a single pair. For example, it is much larger than that in neighboring $^{116}$Xe (Fig. 3). This may suggest that two simultaneous quasiparticle pair alignments occur at $\omega=0.65$ MeV/$\hbar$ for $^{118}$Xe, namely $h_{11/2}$ neutrons [$\omega_{ef}$, see Fig. 4(a)] and $g_{7/2}$ protons [$\omega_{AB}$, see Fig. 4(b)]. However, the neutron $\omega_{ef}$ alignment would have to be significantly delayed (100%) compared to theory. The alignment $i_x$ of $^{118}$Xe is somewhat irregular at the highest spins and may be caused by the influence of further near-yrast noncollective states. Indeed, an oblate state is predicted by the TRS calculations at $I^\pi=48^+$ based on the $\pi[h_{11/2}^2g_{7/2}^2]_{16^+}\otimes\nu[h_{11/2}^4(g_{7/2}/d_{5/2})^{10}]_{32^+}$ configuration.

The $^{116,117}$Xe isotopes do not show the abrupt alignment jump at $\omega_4$. In the case of $^{117}$Xe, the band is observed up to a very high rotational frequency $\omega=1.0$ MeV/$\hbar$ with a gradual stretching out of the $\gamma$-ray spacings [Fig. 2(c)], and consequently a falling moment of inertia. These properties are reminiscent of the behavior of smoothly terminating bands, seen in several neutron-deficient nuclei ($49\leqslant Z\leqslant53$) of this mass region, where a gradual shape change from prolate to oblate takes place over many transitions [3,20]. This is to be contrasted to the abrupt termination seen in $^{117}$I where single yrast oblate states are seen. The smoothly terminating bands are predicted to involve a two-particle two-hole excitation (e.g., $\pi[g_{7/2}^2g_{9/2}^{-2}]$) across the $Z=50$ shell gap. This configuration maintains large prolate deformation at low spin ($\beta_2=0.25-0.30$) and augments the final terminating spin when the oblate shape is achieved. The highest spin observed in $^{117}$Xe, $I^{\pi}=91/2^{-}$, may not represent full termination of the band into an oblate shape. Indeed, TRS calculations suggest a termination spin of $I^{\pi}=99/2^{-}$.

In summary, the yrast bands in $^{116-118}$Xe and $^{117}$I have been significantly extended using highfold $\gamma$-ray coincidence data obtained with the Eurogam II spectrometer. Quasiparticle pair alignments are evident in these bands. The first alignment appears to be due to the rotational alignment of $h_{11/2}$ protons, and consequently the second can be associated with $h_{11/2}$ neutrons. However, theoretical cranking calculations would suggest that the first alignment is caused by $h_{11/2}$ *neutrons* and the second by $h_{11/2}$ *protons*. While the observed proton alignment frequency is slightly lower than theory, the observed neutron alignment frequency is significantly delayed (50% or 180 keV) to higher frequency with respect to theory. Furthermore, the extremely high frequency second alignment in $^{118}$Xe is puzzling. Clearly there is a discrepancy between experiment and theory and these new results highlight inadequacies in the simple cranking model. At the highest spins, contrasting modes of band termination are observed in the $^{117}$I and $^{117}$Xe isobars.

Eurogam is jointly funded by IN2P3 (France) and the EPSRC (United Kingdom). This work was also partly funded by grants from the U.S. National Science Foundation. K.H. acknowledges financial support from the University of York. The authors are indebted to Dr. R. Wyss and Dr. W. Nazarewicz for providing the Woods-Saxon cranking codes.

[1] S. Törmänen *et al.*, Nucl. Phys. **A572**, 417 (1994).
[2] B. Cederwall *et al.*, Z. Phys. A **338**, 461 (1991).
[3] I. Ragnarsson, V.P. Janzen, D.B. Fossan, N.C. Schmeing, and R. Wadsworth, Phys. Rev. Lett. **74**, 3935 (1995).
[4] P.J. Nolan, F.A. Beck, and D.B. Fossan, Annu. Rev. Nucl. Part. Sci. **45**, 561 (1994).
[5] P.M. Jones *et al.*, Nucl. Instrum. Methods (to be published).
[6] D.C. Radford, in *Proceedings of the International Seminar on The Frontier of Nuclear Spectroscopy*, Kyoto, 1992, edited by Y. Yoshizawa, H. Kusakari, and T. Otsuka (World Scientific, Singapore, 1993), p. 229.
[7] C.W. Beausang *et al.*, Nucl. Instrum. Methods (to be published).
[8] K.S. Krane, R.M. Steffen, and R.M. Wheeler, Nuclear Data Tables A **11**, 351 (1973).
[9] M.P. Waring *et al.*, Phys. Rev. C **48**, 2629 (1993).
[10] J. Blachot and G. Marguier, Nucl. Data Sheets **59**, 333 (1990), and references therein.
[11] R. Bengtsson and S. Frauendorf, Nucl. Phys. **A327**, 139 (1979).
[12] S.M. Harris, Phys. Rev. **138**, B509 (1965).
[13] E.S. Paul *et al.*, Phys. Rev. C **45**, R2531 (1992).
[14] R. Wyss, J. Nyberg, A. Johnson, R. Bengtsson, and W. Nazarewicz, Phys. Lett. B **215**, 211 (1988).
[15] W. Nazarewicz, G.A. Leander, and J. Dudek, Nucl. Phys. **A467**, 437 (1987).
[16] W. Nazarewicz, R. Wyss, and A. Johnson, Nucl. Phys. **A503**, 285 (1989).
[17] P.H. Regan *et al.*, Phys. Rev. C **42,** R1805, (1990).
[18] R. Wyss and A. Johnson, in *Proceedings of the International Conference on High-Spin Physics and Gamma-Soft Nuclei*, Pittsburgh, 1990, edited by J.X. Saladin, R.A. Sorensen, and C.M. Vincent (World Scientific, Singapore, 1991), p. 123.
[19] W. Satula, R. Wyss, and F. Dönau, Nucl. Phys. **A565**, 573 (1993).
[20] E.S. Paul *et al.*, Phys. Rev. C **50**, 741 (1994).
[21] S. Juutinen *et al.*, Z. Phys. A **338**, 365 (1991).